P9R.15 Combined Polarimetric and Multiple Doppler Radar Observations of the 16 – 20 March 2003 Colorado Area Winter Storm.

Patrick C. Kennedy*[1], Steven A. Rutledge[1], Gregory S. Poulos[2], and Douglas A. Wesley[3]

[1]Colorado State University, Fort Collins, Colorado
[2]NCAR/EOL, Boulder, Colorado
[3]UCAR/COMET, Boulder, Colorado

1. Introduction

An extensive area of heavy snow (61 - 220 cm; 2 – 7 feet) fell over the eastern foothills of the Rocky Mountains and the adjacent plains regions in Colorado and Southern Wyoming during the 16 – 20 March 2003 period. This precipitation was generated by deep upslope flow produced by an intense low pressure region that moved across southern Colorado. A summary of this winter storm event, including influence of several mesoscale aspects of the storm's organization, are presented in Poulos et al. (2003). This paper is focused on the combined dual-Doppler and dual polarization radar observations that were collected by the CSU-CHILL and Pawnee radars during the passage of one of the storm's snow bands.

2. Dual-Doppler Observations

The data used in this study were collected by two S-Band Doppler research radar systems operated by Colorado State University. The CSU-CHILL radar has a 3dB beam width of 1.0^o and a peak transmitted power of 800 kW. The Pawnee radar has a 1.6^o beam width and a transmitter power of ~400 kW. Both radars use a 1 microsecond pulse duration and a nominal 1 kHZ PRF. To collect dual polarization measurements, the transmitted polarization of the CHILL system was alternated between horizontal and vertical on a pulse-to-pulse basis. The Pawnee radar operated with vertical polarization only. The CHILL radar is located near Greeley, Colorado; the Pawnee radar is located 48 km north northwest of CHILL. The average terrain elevation along the radar baseline is ~1.5 km MSL.

CSU radar operations were undertaken due to the National Weather Service forecasts of a very significant winter storm. A basic scan pattern was devised in which both radars started full PPI volume scans at synchronized 10-minute intervals. The CHILL radar stopped its PPI scans at a maximum elevation of 9^o and executed a series of ~5 RHI scans centered around an azimuth of ~285^o (i.e., towards southern Fort Collins) until the next PPI volume scan start time. The Pawnee radar remained in PPI scan mode and reached a maximum elevation angle of 11^o. With only minor interruptions, the radars remained in this data collection mode from 0114 UTC on March 18 through 0500 UTC on 20 March.

Dual Doppler processing was done using the NCAR SPRINT interpolation (Mohr and Vaughn, 1979) and CEDRIC analysis software (Miller et al., 1986). The Cartesian analysis grid point spacings were 1 km in the horizontal and 0.3 km in the vertical. A series of CEDRIC functions were developed to remove noise and ground clutter contamination from the central analysis region, and to unfold the gridded radial velocities.

A plot of the processed radar data fields at 2.4 km MSL (approximately 1 km AGL above the CSU-CHILL site) at 0504 UTC on 19 March is shown in Figure 1a. According to surface observations, precipitation in the western dual Doppler lobe was composed entirely of snow at this time. (The NWS had issued a blizzard warning for the Fort Collins area at 2340 UTC on 18 March.) The mean motion of the snow band echo was from 070 degrees at 15 ms^{-1}; the band propagated into a region of widespread, fairly steady state, 20-24 dBZ echo that occupied much of the western part of the analysis domain. As indicated by the stream line pattern, the wind direction became more northerly in the barrier jet region (X= -25, Y= 10 km). At the analysis height, the wind speeds in the barrier jet were approximately 20 ms^{-1}; the speeds were 2 – 4 ms^{-1} higher in the northeasterly flow in the eastern dual Doppler lobe. The northerly barrier jet flow was much less evident at heights above ~3 km MSL. At 3.9 km MSL (Fig. 1b), winds were quite generally from the east (i.e., towards higher terrain) over the entire domain. The movement of the snow band echo correlated fairly well with this easterly upper level flow regime.

* *Corresponding author address*: Pat Kennedy, CSU-CHILL Radar, 30750 Weld County Road 45, Greeley, CO 80521; pat@chill.colostate.edu.

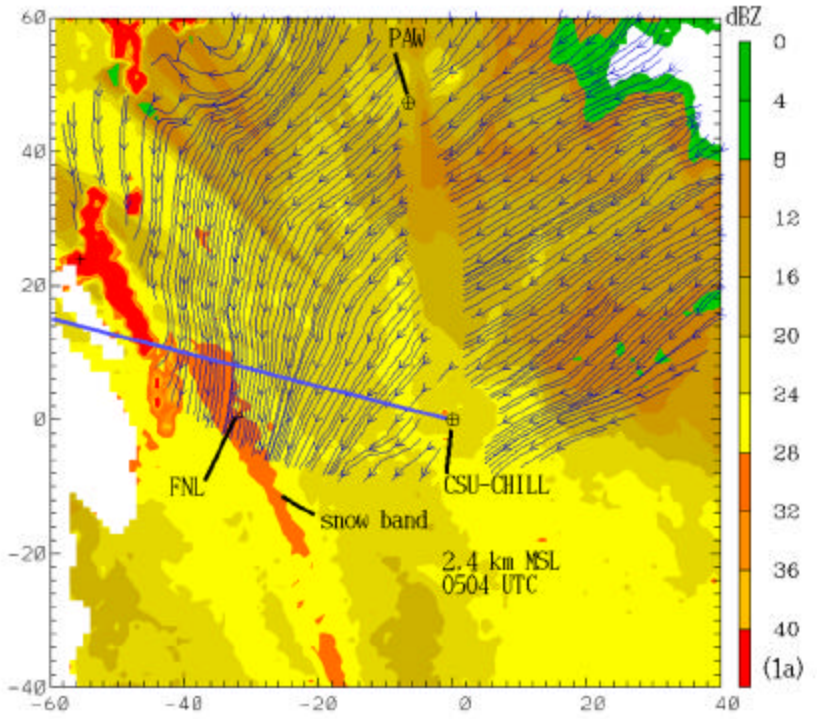

Figure 1a. Streamlines depicting Earth-relative horizontal wind field from a synthesis of the CSU-CHILL and Pawnee radial velocities at 2.4 km MSL. Color filled field is reflectivity in dBZ. Blue line indicates the location of the RHI scans in Figs. 3 and 4. Coordinate axes are in km from an origin at the CSU-CHILL radar. FNL is the Fort Collins-Loveland Municipal Airport.

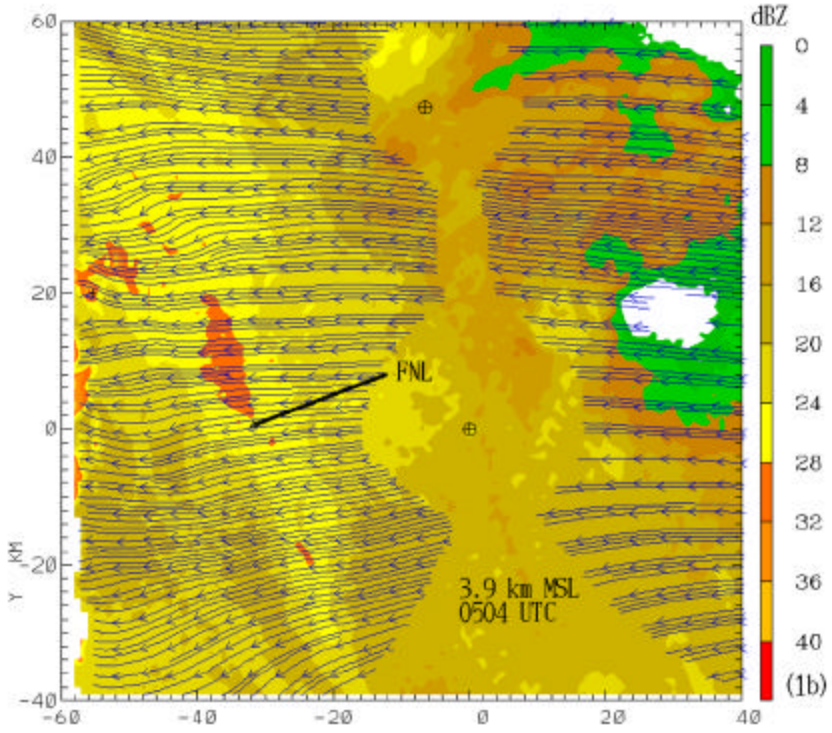

Figure 1b. As in Fig. 1a except the analysis height level is 3.9 km MSL.

The horizontal wind speed magnitudes derived from the dual Doppler wind field components at the 3.9 km height for two analysis times (Figs. 2a and 2b, 0504 and 0454 UTC). The snow band echo's westward propagation is associated with westward expansion of the 18 ms^{-1} wind speed contour at this height. This mesoscale wind speed increase may be a manifestation of gravity wave activity; however, more detailed analyses are necessary to address this possibility. Several aspects of the basic flow patterns seen at 0504 UTC were in a series of dual Doppler analyses done over the 0414 – 0514 UTC period: At low levels, the northerly barrier jet flow remained well established immediately east of the higher terrain. Outside of the barrier jet region, deep, synoptic scale easterly flow existed. The westward advance of an organized area of higher wind speeds at heights around 4 km MSL correlated with the propagation of the primary snow band.

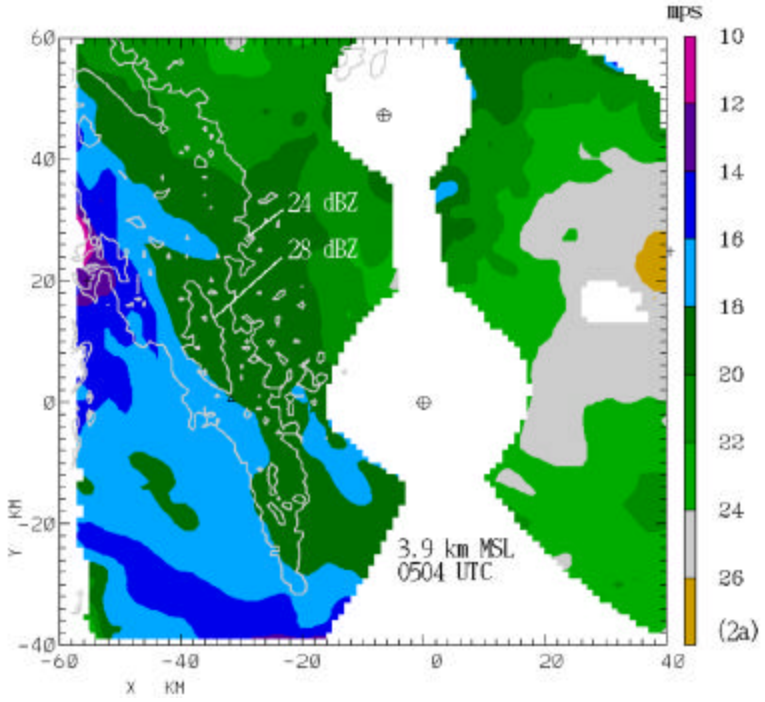

Figure 2a. Horizontal wind speed magnitude at 3.9 km MSL at 0504 UTC computed from the dual-Doppler u and v wind components. (Color filled field; units are ms^{-1}). The snow band location is indicated by the overlaid 24 and 28 dBZ contours.

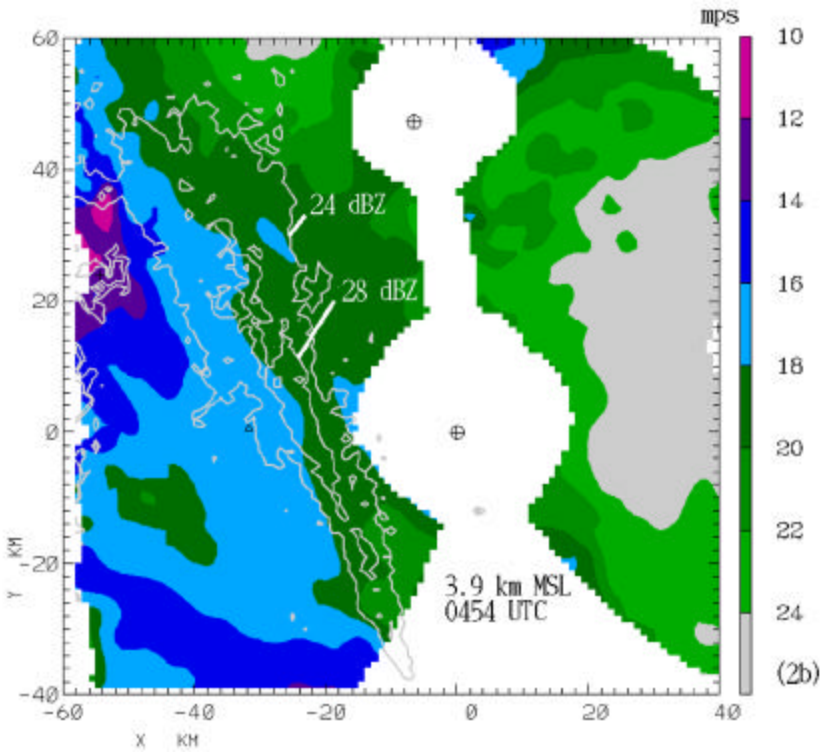

Figure 2b. As in Fig. 2a except time is 0454 UTC.

3. RHI observations

The CSU-CHILL RHI scans intercepted the snow band as it moved through the western dual Doppler lobe shortly before 0500 UTC. At 0452 the snow band was centered near 20 km range in the 285° RHI scan (Fig. 3a). The 28 dBZ contour enclosed a distinct reflectivity core aloft near the 18 km range point. The radial velocity pattern indicated that larger positive (outbound) velocities extended down to lower heights in the area behind the snow band. (Note the vertical compression of the yellow +12 - +15 ms^{-1} color band at ranges shorter than 13 km). A surface-based region of negative (inbound) radial velocities extended westward to the foothills. These negative velocities were due to the inbound flow component that the barrier jet flow projected onto the RHI plane. The differential reflectivity (ZDR; 10 $\log_{10}$ (Z_H/Z_V)) patterns in this RHI plane are shown in Fig. 3b. Positive ZDR values indicate that the preferential orientation of the long axis of the higher reflectivity hydrometeors is quasi-horizontal. Such positive ZDR values existed in a layer between ~1.5 and 4 km AGL ahead of the snow band. ZDR values were generally much closer to 0 dB behind the snow band.

Additional information on particle orientation is provided by specific differential propagation (K_{dp}). K_{dp} expresses the rate at which propagation phase (f_{dp}) differences develop between the horizontally and vertically polarized radar pulses as they move along a common beam path that contains preferentially-oriented hydrometeors. K_{dp} is calculated by determining the range derivative of the basic propagation differential phase (f_{dp}) data values. In this analysis, the K_{dp} calculation procedures used in Cifelli et al. (2002) were applied. The resultant K_{dp} field patterns are shown in Fig. 3c. Slightly positive K_{dp} values (~0.1 to 0.3 deg km^{-1}) exist in an elevated layer ahead of the snow band. K_{dp} values decrease towards zero deg km^{-1} at near-surface heights. Taken together, the combined positive ZDR and K_{dp} values located aloft ahead of the snow band implied that fairly large concentrations of quasi-horizontally-oriented ice crystals were present (Vivekanandan et al., 1994).

These general patterns continued to be evident in the next RHI volume at 0501 UTC (Fig 4). By this time, the elevated reflectivity maximum in the snow band had moved westward to a range of approximately 30 km. K_{dp} values decreased in the area that the snow band had passed through.

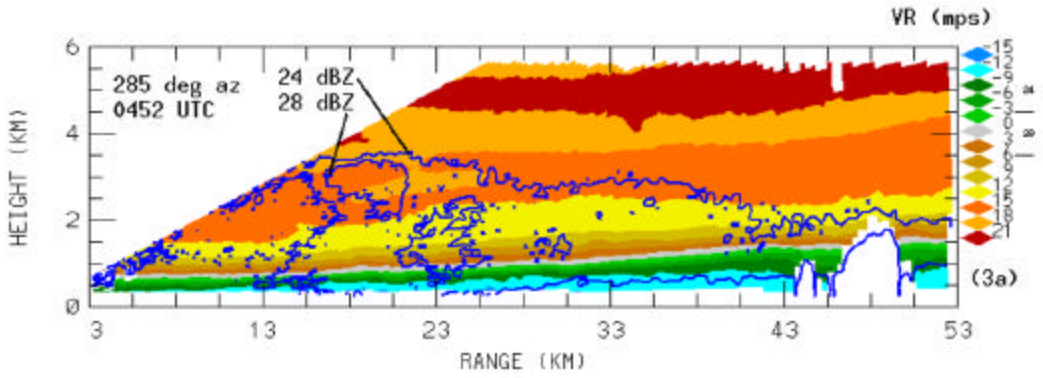

Figure 3a. Radial velocities in the CSU-CHILL 285° RHI plane at 0452 UTC. Outbound velocities are positive. (Color filled field; units are ms^{-1}). The snow band location is shown by the overlaid 24 and 28 dBZ contours. Distances along the axes are in km.

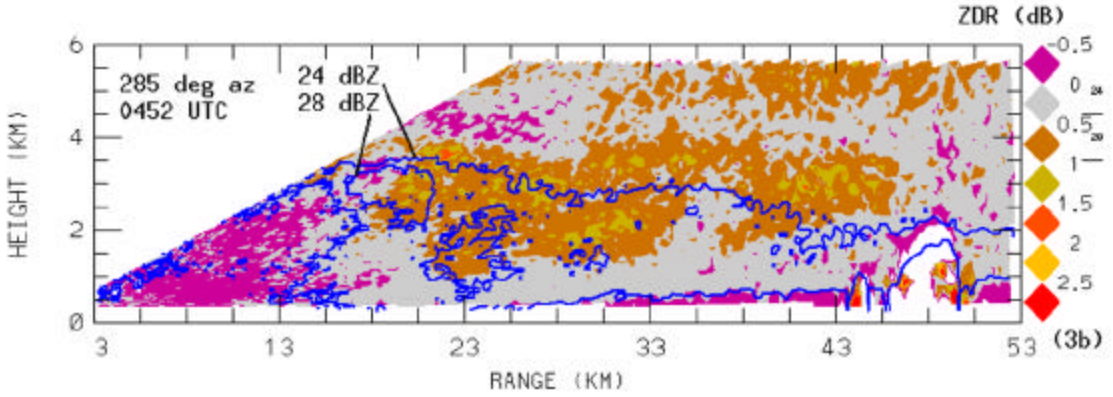

Figure 3. As in Fig. 3a except color filled field is ZDR in dB.

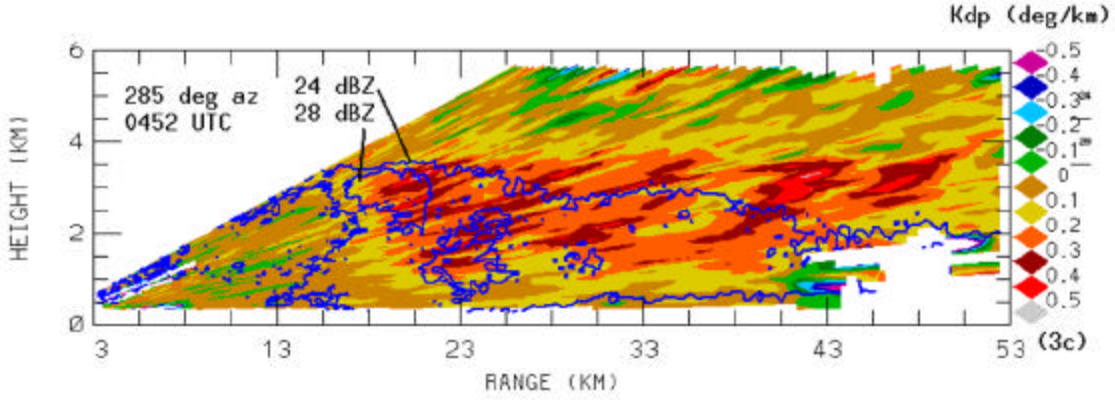

Figure 3c. As in Fig. 3a except color filled field is Kdp in deg km^{-1}.

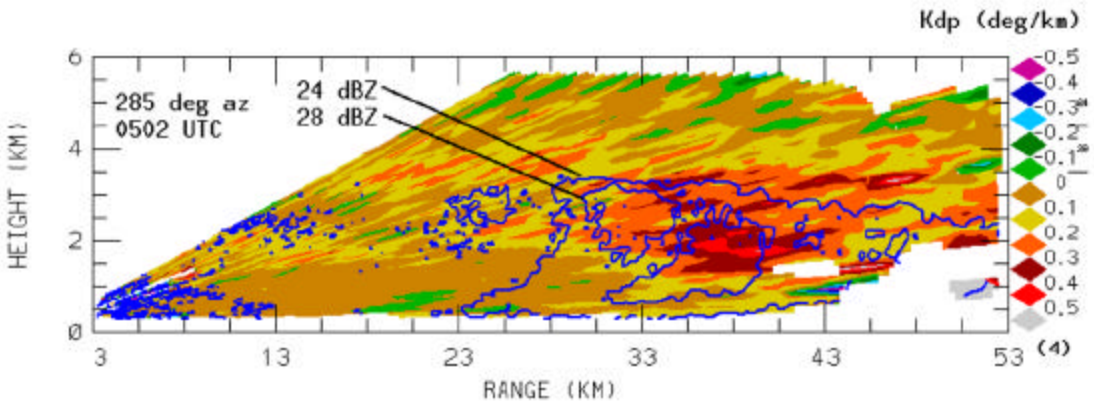

Figure 4. As in Fig. 3c except scan time is 0502 UTC.

4. Particle trajectory calculations

In an effort to connect the polarimetric patterns observed aloft to the low-level snow band echo, particle trajectories were calculated using a program developed at NCAR and outlined in Knight and Knupp (1986). In these calculations, the trajectories are initiated at a prescribed set of grid points within the dual Doppler wind field. The particles are then advected by the time-evolving Doppler-derived wind field. Some parameterization for the particle terminal fall velocities is also required. For the current winter storm case, two modifications were applied to the normal (convective storm) trajectory calculation procedures: The vertical air velocity fields calculated by vertical integration of the divergence field values on the CAPPI planes contained excessive high amplitude noise. The interpolated and filtered radial velocity data still contained enough statistical uncertainty to induce significant local fluctuations in the horizontal divergence fields. This lead to vertical velocity uncertainties of several ms^{-1}; much larger than the ~1 ms^{-1} or less vertical motions that are typical of synoptic scale precipitation systems. For the purposes of this paper, the trajectory calculations were done using a field of randomly distributed vertical air velocities with a mean value of 0 ms^{-1} and a standard deviation of 0.5 ms^{-1}. The second adjustment to the trajectory program input data involved the use of a fixed particle fall speed specification. For simplicity, the snow particles were assigned a constant fall speed of 1 ms^{-1} (Lo, 1982).

To examine the earlier history of the particles that ended up at the lower height levels near the RHI plane, the trajectory calculations were done using a 30 minute sequence of backwards time steps. At this earlier point in time (0434 UTC), most of the particles were located within 250m of the 4.2 km CAPPI height (Fig. 5a). Their horizontal locations at this time were in close proximity to the elevated reflectivity band that was just emerging from the radar baseline area. The ZDR field at the 4.2 km height is shown in Figure 5b. The ZDR pattern at this CAPPI level bears some similarity to that seen in the Figure 3b RHI in that the positive (0.2 – 0.6 dB) ZDR areas are present in much of the region to the west of the snow band. The trajectory points are located in the vicinity of the eastern edge of the positive ZDR area. The corresponding K_{dp} field is shown in Fig. 5c. Positive (0.2 – 0.3^{o} km^{-1}) K_{dp} values are also organized into an elongated region located in close proximity to the leading edge of the snow band (X=35, Y=40 km). The trajectory points are mostly east of this positive K_{dp} band. Thus, at 0434 UTC, the trajectory calculations place the particles towards the rear of the elevated snow band echo and just east of the most positive ZDR and K_{dp} regions.

The trajectory "fallout" locations at the 2.4 km height level 30 minutes later at 0504 UTC are shown in Figure 6. (Since backwards trajectory calculations were done, these are actually the particle launching points). The trajectory results imply that over a 30 minute period, particles that were located just west of the radar base line at 4.2 km MSL have descended into the northerly barrier jet flow and ended up in the low level snow band echo (Fig. 6a). Figure 6b shows the K_{dp} field at "fallout" time. The patterns are similar to those seen at the 4.2 km height 30 minutes earlier (Fig. 5c) in that the >0.2^{o} km^{-1} K_{d}p band is displaced

somewhat ahead of the particle fallout region. During the 30 minute calculation period, many of the trajectory points remain associated with relatively high reflectivities and reduced ZDR and K_{dp} magnitudes. This polarimeteric signal combination is typical of aggregated, low bulk density snow particles (Ryzhkov and Zrnic, 1998).

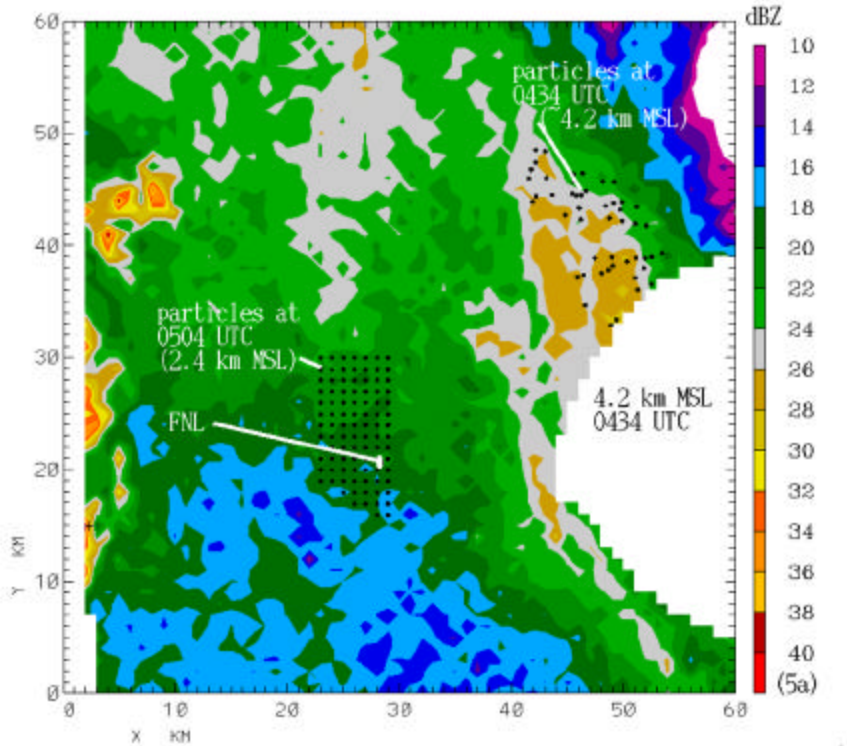

Figure 5a. Reflectivity field at 4.2 km MSL at 0434 UTC. Particle trajectory locations near the 4.2 km and 2.4 km MSL heights are indicated.

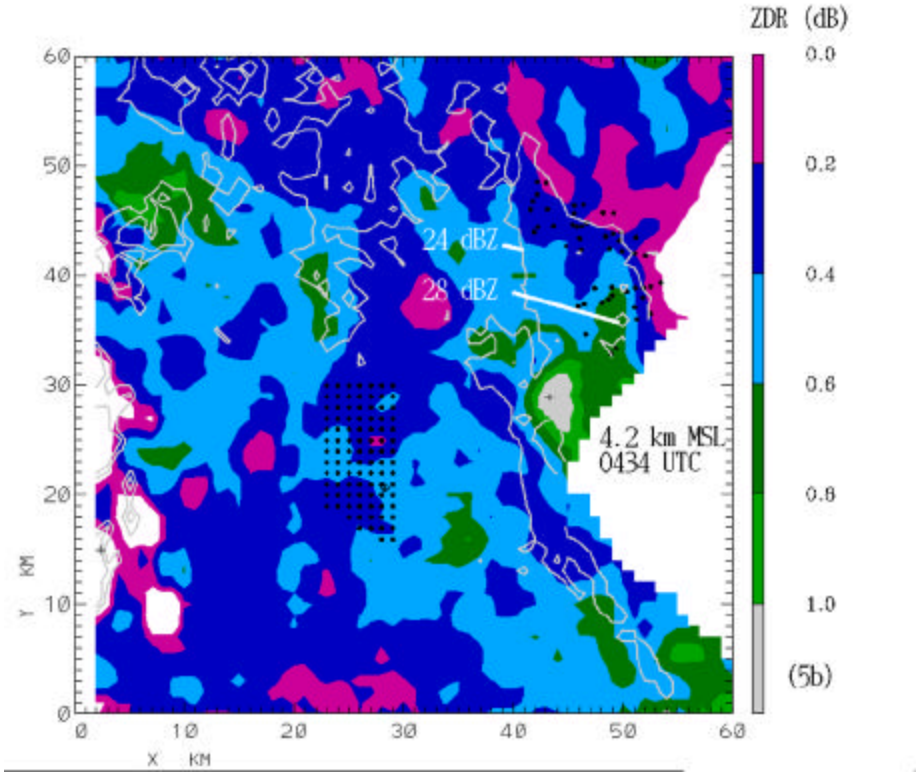

Figure 5b. As in Fig. 5a except color filled field is ZDR in dB. The 24 and 28 dBZ reflectivity contours are overlaid.

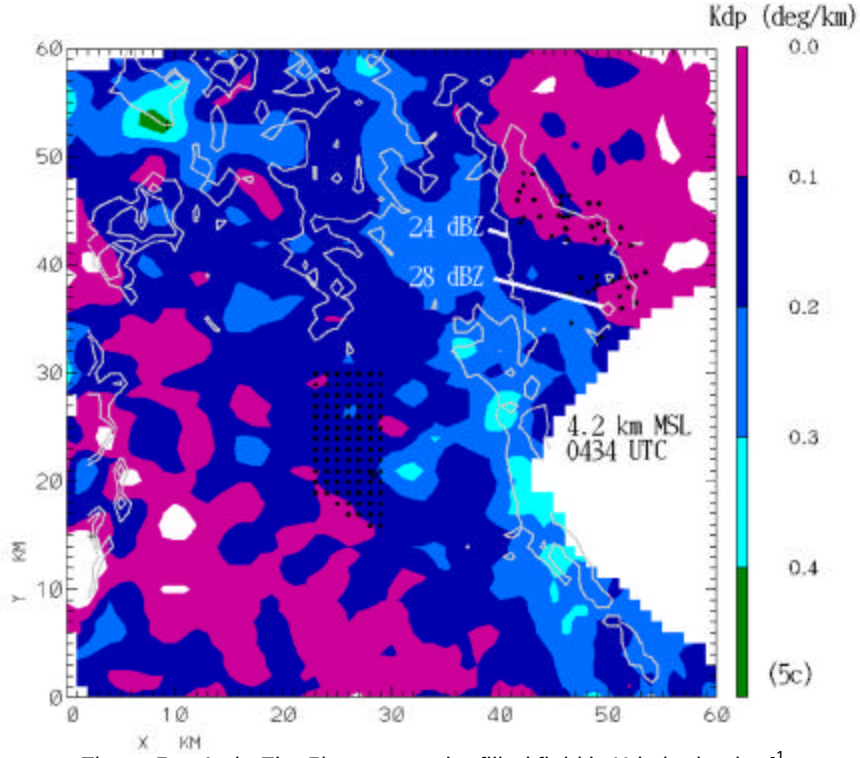

Figure 5c. As in Fig. 5b except color filled field is Kdp in deg km^{-1}.

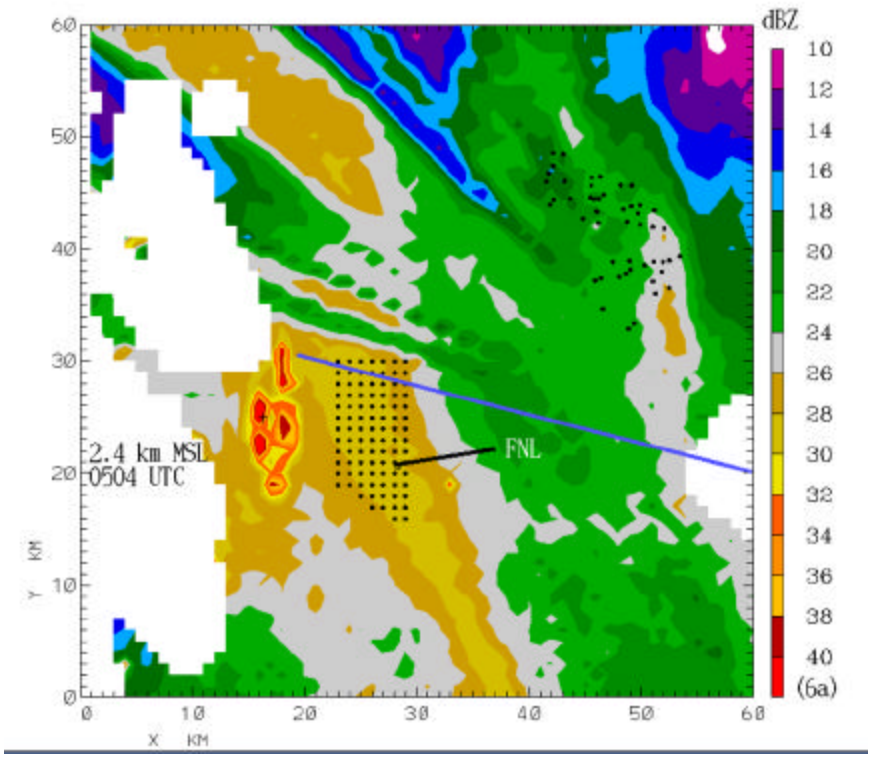

Figure 6a. Reflectivity field at 2.4 km MSL at 0504 UTC. Particle trajectory points as in Fig. 5a.

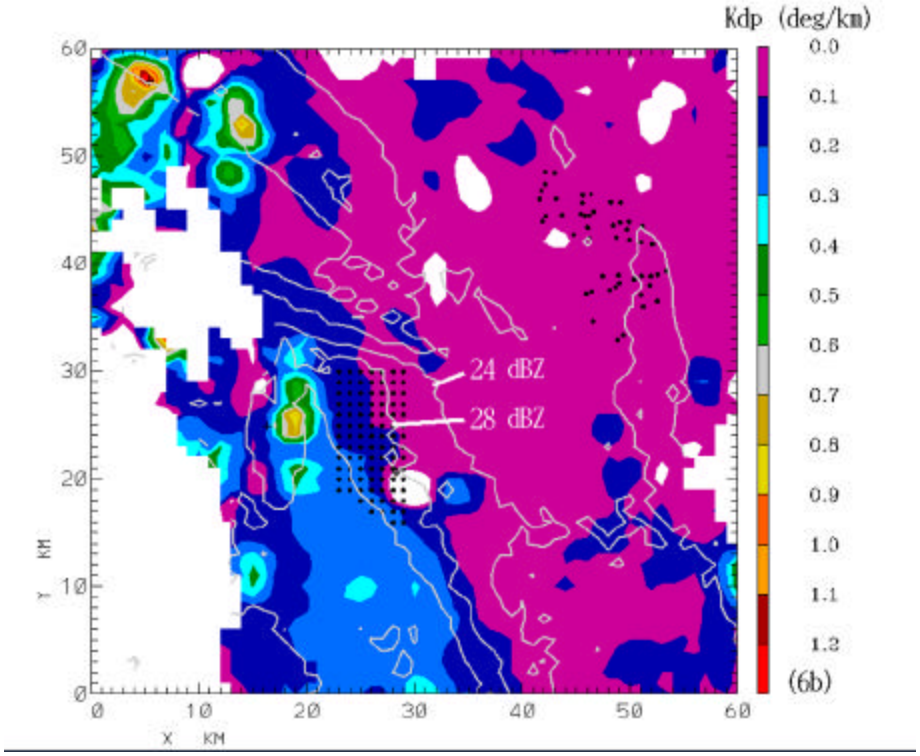

Figure 6b. As in Fig. 6a except color filled field is Kdp in deg km^{-1}. The 24 and 28 dBZ reflectivity contours are overlaid.

5. Discussion

These analyses only present a look at a small segment of a very large winter storm. Within the time period considered here, the horizontal flow fields contained two major components: A synoptic scale easterly flow that extended to the echo tops, and a surface-based northerly barrier jet located immediately east of the Rocky Mountain foothills. As shown most clearly in the RHI data, the depth of this barrier flow increased from east to west. The RHI data also showed that the polarimetric indications of preferential horizontal particle orientations were best defined aloft in the easterly flow region between ~2 to 6 km AGL (approximately –4 to -14^{o} C), probably due to the presence of relatively pristine, un-aggregated ice crystals (Bader et al., 1987).

The snow band echo originated from a generation region that was moving westward in association with the leading edge of an area of stronger horizontal wind speeds at heights above ~2 km AGL. Rather sharp horizontal gradients in the ZDR and K_{dp} fields existed in connection with the snow band echo aloft. The positive values in these polarimeteric fields that were found ahead of the snow band echo diminished rapidly towards the trailing edge of the band. These patterns indicate that snow particle aggregation was locally enhanced in the elevated snow band echo. According to the trajectory calculations, these aggregated particles eventually descended into the low level snow band echo that was stretched out in the northerly barrier jet flow.

Acknowledgements

The radar data processing and display software used in these analyses were developed at and supplied by NCAR. Technical support for the radar operations was provided by David Brunkow and Robert Bowie of the CSU-CHILL radar facility. The CSU-CHILL radar facility is supported by National Science Foundation, cooperative agreement number ATM-0118021.

References

Bader, M.J., S.A. Clough, and G.P. Cox, 1987: Aircraft and dual polarization radar observations of hydrometeors in light stratiform precipitation. *Quart. J. Royal. Meteor. Soc*., **113**, 491-515.

Cifelli, R., W.A. Petersen, L.D. Carey, S.A. Rutledge, and M.A.F. da Silva Dias, 2002: Radar observations of the kinematic, microphysical, and precipitation characteristics of two MCSs in TRMM LBA. *J. Geophys. Res*., **107**, No. D20, 8077

Knight, C.A. and K.R. Knupp, 1986: Precipitation growth trajectories in a CCOPE storm. *J. Atmos. Sci*., **43**, No. 11, 1057-1073.

Miller, L.J., C.G. Mohr, and A.J. Weinheimer, 1986: The simple rectification of Cartesian space of folded radial velocities from Doppler radar sampling. *J. Atmos. Oceanic Tedchnol.*, **3**, 162-174.

Mohr, C.G, and R.L. Vaughn, 1979: An economical procedure for Cartesian interpolation and display of reflectivity data in three-dimensional space. *J. Appl. Meteor*., **18**, 661-670.

Lo, K.K. and R.E. Passarelli, 1982: The growth of snow in winter storms: An airborne observational study. *J. Atmos. Sci*., **39**, No, 4, 697-706.

Poulos, G. S., D. A. Wesley, M. P. Meyers, E. Szoke, and J. S. Snook, 2003: Exceptional mesoscale features of the Great Western Storm of March 16-20, 2003. American Meteorological Society – 10^{th} Conference on Mesoscale Processes, Portland, OR, 23-27 June, paper 14.2A (available in the online permanent archive of the AMS).

Ryzhkov, A.V. and D.S. Zrnic, 1998: Discrimination between rain and snow with a polarimetric radar. *J. Appl. Meteor*., **37**, No. 10, 1228-1240.

Vivekanandan, J., V.N. Bringi, M. Hagen, and P. Mischner, 1994: Polarimetric radar studies of atmospheric ice particles. *IEEE Trans. Geosci. Remote Sens*., **32**, 1-10.